Thermal conductivity and sound attenuation in dilute atomic Fermi gases

Matt Braby, Jingyi Chao, and Thomas Schäfer
Physics Department, North Carolina State University, Raleigh, North Carolina 27695, USA
(Received 22 June 2010; published 27 September 2010)

We compute the thermal conductivity and sound attenuation length of a dilute atomic Fermi gas in the framework of kinetic theory. Above the critical temperature for superfluidity, T_c, the quasiparticles are fermions, whereas below T_c, the dominant excitations are phonons. We calculate the thermal conductivity in both cases. We find that at unitarity the thermal conductivity κ in the normal phase scales as $\kappa \propto T^{3/2}$. In the superfluid phase we find $\kappa \propto T^2$. At high temperature the Prandtl number, the ratio of the momentum and thermal diffusion constants, is 2/3. The ratio increases as the temperature is lowered. As a consequence we expect sound attenuation in the normal phase just above T_c to be dominated by shear viscosity. We comment on the possibility of extracting the shear viscosity of the dilute Fermi gas at unitarity using measurements of the sound absorption length.

DOI: 10.1103/PhysRevA.82.033619 PACS number(s): 03.75.Ss, 05.30.Fk, 05.60.−k, 51.20.+d

I. INTRODUCTION

Cold, dilute Fermi gases in which the interaction between the atoms can be tuned using an external magnetic field provide a new paradigm for strongly correlated quantum fluids [1,2]. Recently, there has been significant interest in the transport properties of these systems [3]. This interest was triggered by three independent developments. The first was the experimental observation of almost ideal hydrodynamic flow in the normal phase of a cold Fermi gas in the limit of infinite scattering length [4]. The second was the discovery of almost ideal flow in a completely different system, the quark-gluon plasma created in heavy-ion collisions at the Relativistic Heavy Ion Collider (RHIC) [5–7]. Both of these experiments constrain the shear viscosity of the fluid. Remarkably, while the absolute value of the shear viscosity of the two systems differs by about 26 orders of magnitude, the ratio of shear viscosity η to entropy density s is very similar, $\eta/s \simeq (0.1\text{–}0.5)\hbar/k_B$, where $\hbar$ is Planck's constant and k_B is Boltzmann's constant [8–12].

The third development was the theoretical discovery of a new method to compute the shear viscosity of strongly coupled field theories [13,14]. This method is based on the holographic duality between four-dimensional field theory and string theory in higher-dimensional spaces [15]. Using the holographic equivalence one can show that in a large class of field theories the strong-coupling limit of η/s is equal to $\hbar/(4\pi k_B) \simeq 0.08\hbar/k_B$. This value is remarkably close to the experimental results for η/s quoted above. Initially the value $\hbar/(4\pi k_B)$ was derived only for scale-invariant relativistic field theories, but it was later shown that the same value of η/s is obtained in the strong-coupling limit of many nonconformal and nonrelativistic field theories [16,17].

In this work we will use kinetic theory to compute another important transport property of a dilute atomic Fermi gas, the thermal conductivity κ. We will consider both the high-temperature and the low-temperature, superfluid, phase. Our results complement earlier studies of the shear and bulk viscosity in the high- and low-temperature phases. The shear viscosity was studied in [18,19]. In the unitarity limit the bulk viscosity of the high-temperature phase vanishes [20]. In the superfluid phase there are three bulk viscosities, one of which is nonvanishing in the unitarity limit. The bulk viscosities in the superfluid phase were recently computed in [21]. Combining our results for the thermal conductivity with the existing calculations of the shear viscosity, we can study the relative size of momentum diffusion and thermal diffusion. The ratio of these quantities is known as the Prandtl number

$$\mathrm{Pr} = \frac{c_P \eta}{\rho \kappa}, \tag{1}$$

where c_P is the specific heat at constant pressure and ρ is the fluid mass density.

The Prandtl number also controls the relative importance of shear viscosity and thermal conductivity in sound attenuation. Measurements of sound attenuation have the potential to provide new experimental constraints on transport properties of dilute atomic gases. Current estimates of the shear viscosity are based on the study of scaling flows, such as collective modes or the expansion out of a deformed trap [10]. These experiments do not directly constrain the density-independent part of the shear viscosity. This is a problem, because kinetic theory predicts that the shear viscosity at high temperature is only a function of temperature, and not of density. Sound attenuation, on the other hand, is sensitive to this contribution. Using our results for the Prandtl number, it is possible to use measurements of sound attenuation to constrain the shear viscosity. Conversely, in the regime where shear viscosity is well constrained it is possible to extract thermal conductivity from sound attenuation. First sound was observed in [22], and ideas for detecting second sound are discussed in [23].

This paper is organized as follows. In Sec. II, we will review the quasiparticle interactions in dilute atomic Fermi gases, and in Sec. III we outline the calculation of thermal conductivity using kinetic theory. In Secs. IV and V we compute the Prandtl number and sound attenuation length. We end with a few comments on the possibility of extracting the sound attenuation length from experiments with optical traps in Sec. VI. Appendix A contains supplementary material regarding the trial functions used for solving the linearized Boltzmann equation, and in Appendix B we collect some thermodynamic relations.

II. ELEMENTARY EXCITATIONS

Kinetic theory is based on the existence of well-defined quasiparticle excitations. In the dilute Fermi gas, quasiparticles

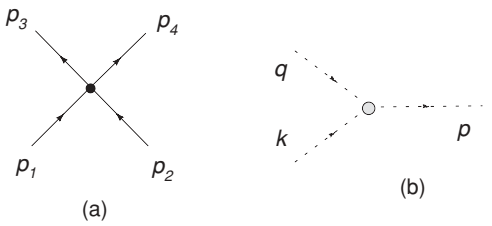

FIG. 1. The main processes that determine the thermal conductivity in the high- and the low- temperature phase, respectively. (a) Shows the local four-fermion interaction, and (b) shows the three-phonon interaction.

exist both at very high and at very low temperature. In the high-temperature limit the relevant degrees of freedom are spin-1/2 nonrelativistic atoms with mass m. In the dilute limit the scattering cross section is dominated by elastic s-wave scattering. The scattering amplitude can be described in terms of a δ-function interaction $V(x-x') = C_0\delta(x-x')$; see Fig. 1. Here, $C_0 = 4\pi a/m$ is related to the scattering length. The s-wave cross section is determined by the sum of all two-body diagrams. The cross section is

$$\sigma = \int d\Omega \frac{a^2}{1+a^2q^2}, \tag{2}$$

where $\boldsymbol{p}_1, \boldsymbol{p}_2$ and $\boldsymbol{p}_3, \boldsymbol{p}_4$ are the ingoing and outgoing momenta and $\boldsymbol{q}$ is the relative momentum $\boldsymbol{q} = (\boldsymbol{p}_1 - \boldsymbol{p}_2)/2$. The relative momentum of the outgoing particles is $\boldsymbol{q}' = (\boldsymbol{p}_3 - \boldsymbol{p}_4)/2$ with $|\boldsymbol{q}'| = |\boldsymbol{q}|$. The solid angle is defined in terms of the angle between the relative momenta $\boldsymbol{q}$ and $\boldsymbol{q}'$, $d\Omega = d\cos(\theta_{\boldsymbol{q}\boldsymbol{q}'})d\phi_{\boldsymbol{q}\boldsymbol{q}'}$.

The characteristic temperature of the system is the Fermi temperature $T_F = k_F^2/(2m)$, where k_F is the Fermi momentum defined by $k_F^3 = 3\pi^2 n_{\rm tot}$ and $n_{\rm tot}$ is the density of both spin states. The strength of the interaction can be characterized by the dimensionless parameter $(k_F a)$. The regime of small and negative $(k_F a)$ is the BCS limit. In this limit the Fermi gas becomes a BCS superfluid at a critical temperature T_c which is exponentially small compared to T_F. The ratio T_c/T_F increases with $|k_F a|$. In the unitary limit $|k_F a| \to \infty$ the critical temperature is $T_c \simeq 0.15 T_F$ [24]. The regime of positive $(k_F a)$ is called the Bose-Einstein condensate (BEC) limit. For small and positive $(k_F a)$ the system is composed of weakly interacting bosons with mass $2m$ and density $n_{\rm tot}/2$. Superfluidity occurs at the Einstein temperature $T_c \simeq 0.21 T_F$.

In the superfluid phase the low-energy excitations are phonons, Goldstone modes associated with the spontaneous breaking of the U(1) phase symmetry. At unitarity the effective Lagrangian for the phonon field is strongly constrained by scale invariance. Son and Wingate showed that [25]

$$\begin{aligned}\mathcal{L}_\phi = {} & \tfrac{1}{2}(\partial_0\phi)^2 - \tfrac{1}{2}v_s^2(\nabla\phi)^2 - g_3\big[(\partial_0\phi)^3 - 9v_s^2\partial_0\phi(\nabla\phi)^2\big] \\ & - \tfrac{3}{2}g_3^2\big[(\partial_0\phi)^4 + 18v_s^2(\partial_0\phi)^2(\nabla\phi)^2 - 27v_s^4(\nabla\phi)^4\big] \\ & + \cdots,\end{aligned} \tag{3}$$

where $g_3 = \pi v^{3/2}\xi^{3/4}/(3^{1/4}8\mu^2)$, μ is the chemical potential, and v_s is the speed of sound given by $v_s^2 = 2\mu/(3m)$. At unitarity $\mu = \xi E_F$ with $\xi \simeq 0.44$ [26]. At low momentum the phonon dispersion relation is linear, $\varepsilon_p = v_s p$. We will see that the thermal conductivity is sensitive to nonlinearities in the dispersion relation. We will write the dispersion relation as $\varepsilon_p = v_s p(1+\gamma p^2)$, where the parameter γ can be expressed in terms of the coefficients of certain higher-order terms in the Lagrangian of Son and Wingate, $\gamma = -\pi^2\sqrt{2\xi}(c_1 + 1.5c_2)/k_F^2$. Rupak and Schäfer computed c_1 and c_2 using an ϵ expansion [27]. They find $c_1 \simeq -\sqrt{2}/(30\pi^2\xi^{3/2})$ and $c_2 \simeq 0$, corresponding to $\gamma = 1/(30m\mu)$. Other estimates of γ can be found in [28–30].

We will study the contribution to thermal conductivity from the phonon splitting process $\varphi \rightleftharpoons \varphi + \varphi$ (see Fig. 1). For $\gamma > 0$ this process is kinematically allowed. The matrix element for the three-phonon process is

$$i\mathcal{M}_3 = g_3[p_0(Q\cdot K) + k_0(Q\cdot P) + q_0(P\cdot K)], \tag{4}$$

where we have defined the four-vector product $Q\cdot K = q_0k_0 - 9v_s^2\boldsymbol{q}\cdot\boldsymbol{k}$. If γ is negative then the dominant contribution arises from $\varphi+\varphi \rightleftharpoons \varphi+\varphi$. We recently studied this process in a relativistic superfluid, the color-flavor-locked phase of QCD [31]. We found that the $2 \rightleftharpoons 2$ processes are controlled by s,t,u-channel exchanges with almost on-shell intermediate state phonons. This means that the dominant process can be viewed as $1 \leftrightharpoons 2$ phonon splitting followed by $2 \leftrightharpoons 1$ phonon absorption.

III. THERMAL CONDUCTIVITY

Thermal conductivity is defined by the relation between the heat current $\boldsymbol{h}$ and the temperature gradient, $\boldsymbol{h} = -\kappa\nabla T$. In kinetic theory the heat current is expressed in terms of the quasiparticle distribution function,

$$\boldsymbol{h} = \nu\int d\Gamma\, \varepsilon_p \boldsymbol{v}_p \delta f_p \tag{5}$$

where ν is the degeneracy factor, $d\Gamma = d^3p/(2\pi)^3$, $\boldsymbol{v}_p$ is the particle velocity, and δf is the deviation of the distribution function from its equilibrium value, $\delta f = f - f^0$, with $f_0(p) = 1/(e^{(\varepsilon_p-\mu)/T} \pm 1)$ for bosons and fermions, respectively. Note that in the case of phonons there is no conserved particle number and $\mu = 0$. The correction to the distribution function is linear in ∇T, and we can define

$$\delta f_p = -\frac{f_0(p)\,[1 \pm f_0(p)]}{T^2}\boldsymbol{\chi}\cdot\nabla T. \tag{6}$$

With this form we can rewrite Eq. (5) as

$$\begin{aligned}\boldsymbol{h} &= -\frac{\nu\nabla T}{3T^2}\int d\Gamma\, \varepsilon_p\, \boldsymbol{v}_p\cdot\boldsymbol{\chi}\, f_0(p)\,[1\pm f_0(p)] \\ &\equiv -T\nabla T\,\langle \varepsilon_p\, \boldsymbol{v}_p|\boldsymbol{\chi}\rangle,\end{aligned} \tag{7}$$

where we have defined an inner product as

$$\langle \boldsymbol{a}|\boldsymbol{b}\rangle = \frac{\nu}{3T^3}\int d\Gamma\, f_0(p)\,[1\pm f_0(p)]\boldsymbol{a}\cdot\boldsymbol{b}. \tag{8}$$

We can then write the thermal conductivity as

$$\kappa = T\,\langle \varepsilon_p\, \boldsymbol{v}_p|\boldsymbol{\chi}\rangle. \tag{9}$$

There are certain constraints on the the form of $\boldsymbol{\chi}$. The Boltzmann equation conserves energy, momentum, and, in the case of a conserved charge, particle number. A nontrivial

constraint on $\boldsymbol{\chi}$ arises due to momentum conservation. We have

$$0 = \nu \int d\Gamma\, \boldsymbol{p}\, \delta f_p = -\frac{\nu}{T^2} \int d\Gamma\, \boldsymbol{p}(\boldsymbol{\chi}\cdot\boldsymbol{\nabla} T) f_0(p)\,[1 \pm f_0(p)] = -T\boldsymbol{\nabla} T \langle \boldsymbol{p}|\boldsymbol{\chi}\rangle, \tag{10}$$

which implies that $\langle \boldsymbol{p}|\boldsymbol{\chi}\rangle = 0$. As we can see from the constraint and Eq. (9), any term in $\varepsilon_p \boldsymbol{v}_p$ that is linear in $\boldsymbol{p}$ will not contribute to the thermal conductivity. In particular, if the kinetic description is governed by a quasiparticle with exactly linear dispersion relation then the thermal conductivity vanishes.

The function $\boldsymbol{\chi}$ is determined by solving the Boltzmann equation

$$\frac{df}{dt} = \frac{\partial f}{\partial t} + \boldsymbol{v}_p \cdot \boldsymbol{\nabla} f = C[f], \tag{11}$$

where $C[f]$ is the collision integral. Schematically we can write

$$C[f] = \int d\Gamma_{n-1}\, w(\text{in};\text{out}) D_{\text{in}\leftrightarrow\text{out}}, \tag{12}$$

where $d\Gamma_{n-1}$ is the $(n-1)$-particle phase space (all the particles not labeled by momentum p), w is the transition probability, and $D_{\text{in}\leftrightarrow\text{out}}$ contains the distribution functions. Taking the convective derivative on the left-hand side of the Boltzmann equation and focusing only on terms proportional to the temperature gradient, we can write

$$\frac{df}{dt} = \frac{f_0(1\pm f_0)}{3T}\boldsymbol{\alpha}_p \cdot \boldsymbol{\nabla} T \equiv \frac{f_0(1\pm f_0)}{3T}|\boldsymbol{\alpha}_p\rangle \cdot \boldsymbol{\nabla} T, \tag{13}$$

where $\boldsymbol{\alpha}_p$ will depend on equilibrium properties of the quasiparticle system. In the case of either particles with linear dispersion (like phonons) or particles with nonrelativistic dispersions and a chemical potential, we can write [31]

$$\boldsymbol{\alpha}_p \sim \frac{\varepsilon_p \boldsymbol{v}_p}{T} + A\boldsymbol{p}, \tag{14}$$

where A depends only on the thermodynamics of the system. We can linearize the right-hand side of Eq. (11) in $\boldsymbol{\chi}$ as

$$C[f] = C[f_0] + C[\delta f] = C[\delta f] = \int d\Gamma\, w(\text{in};\text{out}) \delta D_{\text{in}\leftrightarrow\text{out}} \equiv \frac{f_0(1\pm f_0)}{3T}\hat{C}|\boldsymbol{\chi}\rangle \cdot \boldsymbol{\nabla} T, \tag{15}$$

where we have defined the linearized collision operator $\hat{C}$ acting on the state $|\boldsymbol{\chi}\rangle$. We will specify $\hat{C}$ in more detail below. We can now write the linearized Boltzmann equation as

$$|\boldsymbol{\alpha}_p\rangle = \hat{C}|\boldsymbol{\chi}\rangle. \tag{16}$$

The thermal conductivity is now determined by solving Eq. (16) for $|\boldsymbol{\chi}\rangle$ and then computing κ using Eq. (9). In practice, we will adopt a variational procedure. Using the constraint we can show that $T\langle \boldsymbol{\chi}|\boldsymbol{\alpha}_p\rangle = \langle \varepsilon_p \boldsymbol{v}_p|\boldsymbol{\chi}\rangle$ for both fermions and bosons. The thermal conductivity can then be written in two alternative ways:

$$\kappa = T\langle \varepsilon_p \boldsymbol{v}_p|\boldsymbol{\chi}\rangle \quad \text{and} \quad \kappa = T^2\langle \boldsymbol{\chi}|\hat{C}|\boldsymbol{\chi}\rangle, \tag{17}$$

where we have used the Boltzmann equation, Eq. (16), to derive the second equality. These two representations form the basis of the variational principle. Consider a trial state $|\boldsymbol{g}\rangle$. The Schwarz inequality implies that

$$\langle \boldsymbol{g}|\hat{C}|\boldsymbol{g}\rangle\langle \boldsymbol{\chi}|\hat{C}|\boldsymbol{\chi}\rangle \geqslant |\langle \boldsymbol{g}|\hat{C}|\boldsymbol{\chi}\rangle|^2. \tag{18}$$

Using Eq. (17) and Eq. (16), we can write this as

$$\kappa \geqslant T^2 \frac{|\langle \boldsymbol{g}|\boldsymbol{\alpha}_p\rangle|^2}{\langle \boldsymbol{g}|\hat{C}|\boldsymbol{g}\rangle} = \frac{|\langle \boldsymbol{g}|\varepsilon_p \boldsymbol{v}_p\rangle|^2}{\langle \boldsymbol{g}|\hat{C}|\boldsymbol{g}\rangle}. \tag{19}$$

Using Eq. (17) we observe that an exact solution of the linearized Boltzmann equation saturates the inequality. We can then choose to expand the trial function $\boldsymbol{g}$ in orthogonal polynomials and take advantage of the fact that $\boldsymbol{g}$ is a dimensionless vector-valued function to write

$$\boldsymbol{g} = \boldsymbol{x} \sum_{s\neq 0}^{N} b_s^{(F,H)} B_s^{(F,H)}(x^2), \tag{20}$$

where $\boldsymbol{x} = \boldsymbol{p}/\Delta$, $x = |\boldsymbol{x}|$, and Δ is some characteristic energy scale in the problem (e.g., $\Delta = T/v_s$ for massless particles and $\Delta = \sqrt{2mT}$ for massive particles). The polynomials are such that $B_0 = 1, B_1 = x^2 + a_{10}$, $B_2 = x^4 + a_{21}x^2 + a_{20}$, etc., and (F,H) labels the basis functions in the fermion and phonon case. The orthogonality condition is

$$A_s^{(F,H)}\delta_{st} = \int dx f_0(x)\,[1 \pm f_0(x)] x^4 B_s^{(F,H)}(x^2) B_t^{(F,H)}(x^2). \tag{21}$$

The type of quasiparticle involved enters via the statistical factor $[1 \pm f_0(x)]$ and through the dispersion relation in $f_0(x)$. The specific forms of $B_m^{(F,H)}(x^2)$ are given in Appendix A. Note that we have enforced the momentum constraint by excluding the $s = 0$ term in Eq. (20).

A. Normal phase

In this section we will specify the matrix elements and the collision operator in the case of atom-atom scattering in the normal phase of the dilute Fermi gas. We will scale all the momenta as $x_i = p_i/\sqrt{2mT}$, use the Fermi-Dirac distribution functions, and set $\nu = 2$. The numerator of Eq. (19) is

$$\begin{aligned}\langle \boldsymbol{g}|\varepsilon_p \boldsymbol{v}_p\rangle &= \frac{2}{3T^3}\int d\Gamma\, f_0(p)\,[1 - f_0(p)]\varepsilon_p \boldsymbol{v}_p \cdot \boldsymbol{g} \\ &= \frac{4m}{3\pi^2}\sum_{s\neq 0} b_s^F \int dx\, f_0(x)\,[1 - f_0(x)] x^6 B_s^F(x^2) \\ &= \frac{4m}{3\pi^2}\sum_{s\neq 0} b_s^F A_{s1}^F \delta_{s1} = \frac{4m}{3\pi^2} b_1^F\, A_{11}^F,\end{aligned} \tag{22}$$

where we have used the orthogonality condition. The matrix element of the collision operator is

$$\langle \boldsymbol{g}|\hat{C}|\boldsymbol{g}\rangle = \frac{2}{3T^4}\sum_{s,t\neq 0} b_s^F b_t^F \int \frac{d^3P d^3q}{(2\pi)^6}\, d\Omega |\boldsymbol{v}_1 - \boldsymbol{v}_2| \frac{a^2}{1 + a^2 q^2} \times D^0_{2\leftrightarrow 2} \boldsymbol{g}_1 \cdot (\boldsymbol{g}_1 + \boldsymbol{g}_2 - \boldsymbol{g}_3 - \boldsymbol{g}_4). \tag{23}$$

Here we have written the transition probability in terms of the cross section Eq. (2) and the flux factor $|\boldsymbol{v}_1 - \boldsymbol{v}_2|$. The integration variables are the pair momentum $\boldsymbol{p} = \boldsymbol{p}_1 + \boldsymbol{p}_2$, the relative momentum $\boldsymbol{q} = (\boldsymbol{p}_1 - \boldsymbol{p}_2)/2$, and the solid angle

Ω defined below Eq. (2). We have also defined $D^0_{2\leftrightarrow 2} = f_0(x_1)f_0(x_2)[1-f_0(x_3)][1-f_0(x_4)]$. We can write

$$\langle \boldsymbol{g}|\hat{C}|\boldsymbol{g}\rangle = \frac{2^{11/2}m^{3/2}}{3T^{3/2}}\sum_{s,t\neq 0} b_s^F b_t^F \int \frac{d^3x d^3y}{(2\pi)^6} d\Omega \frac{mTa^2y}{1+2mTa^2y^2} \times D^0_{2\leftrightarrow 2}\boldsymbol{B}_s^F\cdot\boldsymbol{B}_t^F = \frac{2^{11/2}m^{3/2}}{3T^{3/2}}\sum_{s,t\neq 0} b_s^F b_t^F M_{st}^F, \tag{24}$$

where $x=|\boldsymbol{P}|/\sqrt{2mT}$, $y=|\boldsymbol{q}|/\sqrt{2mT}$, and $\boldsymbol{B}_t^F = [B_t^F(x_1)\boldsymbol{x}_1 + B_t^F(x_2)\boldsymbol{x}_2 - B_t^F(x_3)\boldsymbol{x}_3 - B_t^F(x_4)\boldsymbol{x}_4]/2$. We finally get

$$\kappa_F \geqslant \frac{\langle \boldsymbol{g}|\varepsilon_p \boldsymbol{v}_p\rangle^2}{\langle \boldsymbol{g}|\hat{C}|\boldsymbol{g}\rangle} = \frac{\kappa_0}{3\times 2^{3/2}\pi^4}\left(\frac{T}{T_F}\right)^{3/2} D_F(k_F a, T/T_F), \tag{25}$$

where we have defined $\kappa_0 = m^{1/2}T_F^{3/2}$ and

$$D_F(k_F a, T/T_F) \equiv \frac{\left(b_1^F\right)^2\left(A_{11}^F\right)^2}{\sum_{s,t\neq 0} b_s^F b_t^F M_{st}^F}. \tag{26}$$

We can now consider a finite basis and optimize the inequality with respect to the coefficients b_s^F. We obtain $D_F(k_F a, T/T_F) = (A_{11}^F)^2 (M^F)^{-1}_{11}$ where $(M^F)^{-1}_{11}$ refers to the (1,1) component of the matrix inverse of M. Note that this result is equivalent to using the matrix form of the Boltzmann equation in a finite basis. The function D_F must typically be calculated numerically. We can analytically evaluate D_F in the limit of high temperature $T/T_F \gg 1$ and by keeping only the leading term in the polynomial expansion. We get

$$\kappa_F = \begin{cases} \frac{75}{128\sqrt{\pi}}\sqrt{\frac{T}{m}}\frac{1}{a^2}, & |a|\to 0, \\ \frac{225}{128\sqrt{\pi}} m^{1/2}T^{3/2}, & |a|\to\infty. \end{cases} \tag{27}$$

We have tried to improve this result using higher-order terms in the polynomial expansion, but the correction is very small, $\delta\kappa/\kappa < 2\%$. This is consistent with the results in [32], where the authors observed very rapid convergence for the shear viscosity in the high-temperature phase. Numerical results are shown in Fig. 2. Note that the thermal conductivity depends only on the square of the scattering length so we plot the thermal conductivity as a function of $k_F|a|$. We observe that,

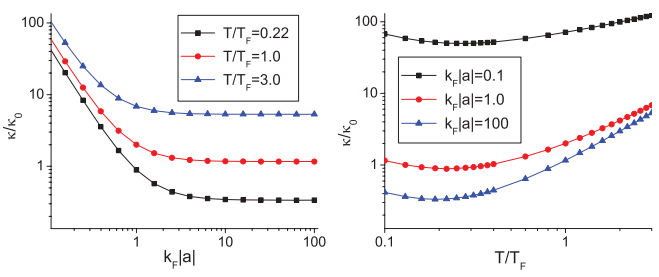

FIG. 2. (Color online) Thermal conductivity in the normal phase of a dilute Fermi gas in units of $\kappa_0 = m^{1/2}T_F^{3/2}$. In the left panel we show κ/κ_0 as a function of T/T_F for different values of $k_F a$. In the right panel we show κ/κ_0 as a function of $k_F a$ for different values of T/T_F.

qualitatively, the temperature dependence of κ is the same for all values of $k_F|a|$. In the unitarity limit, κ grows as $\sim T^{3/2}$ for $T \gg T_F$. In the BCS limit the temperature dependence is $\kappa \sim T^{1/2}$. The thermal conductivity has a minimum at $T/T_F \simeq$ (0.2–0.3), and increases for very small temperatures. This rise is related to Pauli blocking. We should note, however, that except in the BCS limit the results in this section are not reliable for $T \ll T_F$. The right panel shows that at fixed temperature κ decreases as the strength of the interaction increases, and that κ becomes insensitive to $k_F a$ as we approach the unitarity limit $k_F a \to \infty$.

B. Superfluid phase

In this section we study the thermal conductivity in the superfluid phase. We will concentrate on the unitarity limit $k_F a \to \infty$. In the BCS limit the critical temperature is exponentially small, and the thermal conductivity is dominated by fermionic quasiparticles even in the case $T < T_F$. In the extreme BEC limit the thermal conductivity reduces to that of an almost ideal Bose gas [33]. Following the procedure outlined in the case of the normal phase, we can write the numerator of Eq. (19) as

$$\langle \boldsymbol{g}|\varepsilon_p\boldsymbol{v}_p\rangle = \frac{1}{3T^3}\int d\Gamma f_0(p)[1+f_0(p)]\varepsilon_p\boldsymbol{v}_p\cdot\boldsymbol{g} = \frac{2\gamma}{3\pi^2}\frac{T^3}{v_s^4}\sum_{s\neq 0} b_s^H \int dx f_0(x)[1+f_0(x)]x^6 B_s^H(x^2) = \frac{2\gamma}{3\pi^2}\frac{T^3}{v_s^4} b_1^H A_{11}^H, \tag{28}$$

where we have used $v=1$, scaled the momenta as $x = vp/T$, and kept only the leading-order terms in the parameter γ that governs nonlinearities in the dispersion relation. We note that the result is indeed proportional to γ, and κ vanishes in the case of an exactly linear dispersion relation as discussed before. The matrix element of the collision operator is

$$\langle \boldsymbol{g}|\hat{C}|\boldsymbol{g}\rangle = \frac{1}{3T^4}\sum_{s,t\neq 0} b_s^H b_t^H \int d\Gamma_{pkq}|\mathcal{M}_3(p,k,q)|^2(2\pi)^4 \times \delta^4(P+K-Q)D^0_{1\leftrightarrow 2}\boldsymbol{B}_s^H\cdot\boldsymbol{B}_t^H = \frac{g_3^2}{96\pi^3}\frac{T^5}{v_s^6}\sum_{s,t\neq 0} b_s^H b_t^H \int d\Gamma_{xyz}|\mathcal{M}_3(x,y,z)|^2(2\pi)^4 \times \delta^4(X+Y-Z)D^0_{1\leftrightarrow 2}\boldsymbol{B}_s^H\cdot\boldsymbol{B}_t^H = \frac{g_3^2}{96\pi^3}\frac{T^5}{v_s^6}\sum_{s,t\neq 0} b_s^H b_t^H M_{st}^H, \tag{29}$$

where $d\Gamma_{pkq}$ is the three-particle Lorentz-invariant phase space, $X=(x_0,\boldsymbol{x}) = (p_0/T, v_s\boldsymbol{p}/T)$, etc., $D^0_{1\leftrightarrow 2} = f_0(x)f_0(y)[1+f_0(z)]$, and $\boldsymbol{B}_t^H = [B_t^H(x)\boldsymbol{x} + B_t^H(y)\boldsymbol{y} - B_t^H(z)\boldsymbol{z}]/\sqrt{3}$. As before, we can define

$$D_H = \left(A_{11}^H\right)^2\left(M_{st}^H\right)^{-1}_{11}, \tag{30}$$

which allows us to write the thermal conductivity as

$$\kappa_H \geqslant \frac{\langle \boldsymbol{g}|\varepsilon_p\boldsymbol{v}_p\rangle^2}{\langle \boldsymbol{g}|\hat{C}|\boldsymbol{g}\rangle} = \frac{128}{3\pi}\frac{\gamma^2}{g_3^2}\frac{T^2}{v_s^2}D_H = \frac{256\sqrt{2}}{25\pi^3\xi^2}\kappa_0\left(\frac{T}{T_F}\right)^2 D_H(T/T_F), \tag{31}$$

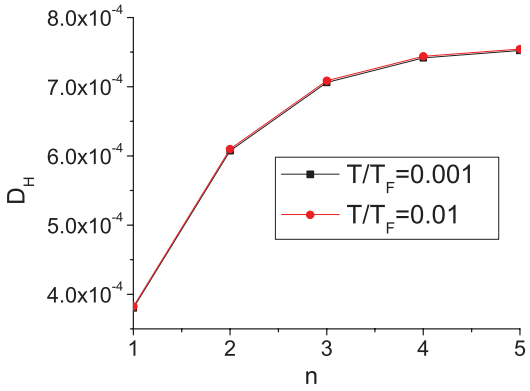

FIG. 3. (Color online) Variational function D_H as a function of the number of terms in the polynomial expansion of $\tilde{g}(x)$. We show D_H for two different temperatures.

where $\xi \simeq 0.44$ is defined in Sec. II. D_H is a dimensionless function of T/T_F that has to be calculated numerically. The convergence of D_H with the number of terms in the trial function is shown in Fig. 3. We observe that the result is converging, but not nearly as fast as it did in the case of fermionic quasiparticles. The temperature dependence of D_H is very weak and $\kappa_H \sim T^2$. In Fig. 4 we combine our results for the thermal conductivity of the dilute Fermi gas at unitarity in the high- and low-temperature limits. The dashed line indicates the location of the phase transition. We note that the low- and high-temperature results do not match very well near T_c. This suggests that additional processes or excitations must become relevant in this regime. We also note that at T_c critical fluctuations are expected to lead to a divergence in the thermal conductivity [34].

IV. SHEAR VISCOSITY AND THE PRANDTL NUMBER

A. Shear viscosity

In order to compare the magnitude of thermal and momentum diffusion in dilute atomic gases, we also need to determine the viscosity of the gas. The shear viscosity of the dilute Fermi gas at unitarity has been calculated in both

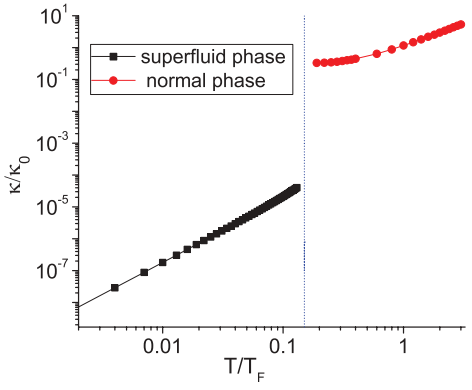

FIG. 4. (Color online) Thermal conductivity κ/κ_0 of the dilute Fermi gas at unitarity as a function of T/T_F. We show the calculations in the high- and low-temperature limits, extrapolated to $T \simeq T_c$. The position of the critical temperature is indicated by the dashed line.

the high-temperature [18] and low-temperature limits [19]. Here, we quickly summarize the results and present a simple numerical formula that can be used to compute the contribution from binary scattering of atoms for all values of $k_F a$ and T/T_F.

The viscous correction to the stress tensor is

$$\delta T_{ij} = \nu \int d\Gamma v_p \frac{p_i p_j}{p} \delta f_p = -\eta V_{ij}, \tag{32}$$

where $V_{ij} = \partial_i V_j + \partial_j V_i - 2/3 \delta_{ij} \nabla \cdot \boldsymbol{V}$ and V_i is the velocity of the fluid. We use an ansatz for δf_p analogous to the one that appeared in the calculation of the thermal conductivity,

$$\delta f_p = -\frac{f_0(p)[1 \pm f_0(p)]}{T} \chi_{ij} V_{ij}. \tag{33}$$

The shear viscosity η is then given by

$$\eta = \frac{\nu}{5T} \int d\Gamma f_0(p)[1 \pm f_0(p)] \frac{v_p}{p} p_i p_j \chi_{ij} \equiv \frac{3T^2}{5} \langle \tilde{p}_{ij} | \chi_{ij} \rangle, \tag{34}$$

where $\tilde{p}_{ij} = v_p (p_i p_j - \frac{1}{3} \delta_{ij} p^2)/p$ and we have used the inner product defined previously. The linearized Boltzmann equation for a fluid perturbed by a small shear stress is given by

$$\frac{df}{dt} = \frac{f_0(p)[1 \pm f_0(p)]}{2T} |\tilde{p}_{ij}\rangle V_{ij}$$
$$= C[f_p] \equiv \frac{f_0(p)[1 \pm f_0(p)]}{2T} \hat{C} |\chi_{ij}\rangle V_{ij}. \tag{35}$$

As before, we can combine these results into a form that is suitable for a variational treatment. We write

$$\eta = \frac{3T^2}{5} \frac{\langle \chi_{ij} | \tilde{p}_{ij} \rangle^2}{\langle \chi_{ij} | \hat{C} | \chi_{ij} \rangle} \tag{36}$$

and $\chi_{ij} = \frac{p_{ij}}{\Delta^2} \tilde{g}(x)$. We expand $\tilde{g}(x) = \sum_{s=0} c_s C_s(x^2)$ where the polynomials $C_s(x^2)$ are defined in analogy with Eq. (21) but with the weight factor x^4 replaced by x^6 (see Appendix A). In the case of binary atomic scattering the variational bound is

$$\eta_F \geqslant \frac{2^{7/2} \eta_0}{45} \left(\frac{T}{T_F} \right)^{3/2} D^\eta(k_F a, T/T_F), \tag{37}$$

where $\eta_0 = (m T_F)^{3/2}$ and $D^\eta(k_F a, T/T_F) = (A_0^\eta)^2 (M^\eta)^{-1}_{00}$. The normalization integral is

$$A_0^\eta = \int dx f_0(x)[1 - f_0(x)] x^6 = z \int dx\, x^6 \frac{e^{x^2}}{\left(e^{x^2} + z\right)^2}, \tag{38}$$

where $z = e^{\mu/T}$ is the fugacity and the collision matrix elements M_{st}^η are given by

$$M_{st}^\eta = \int \frac{d^3x d^3y}{(2\pi)^6} d\Omega \frac{m T a^2 y}{1 + 2 m T a^2 y^2} D^0_{2 \leftrightarrow 2} \widehat{C}_s \cdot \widehat{C}_t \tag{39}$$

with $D^0_{2\leftrightarrow 2} = f_0(x_1) f_0(x_2)[1 - f_0(x_3)][1 - f_0(x_4)]$ and

$$\widehat{C}_t = \left[C_t(x_1) x_1^{ij} + C_t(x_2) x_2^{ij} - C_t(x_3) x_3^{ij} - C_t(x_4) x_4^{ij} \right]/2. \tag{40}$$

As in the case of thermal conductivity, we can analytically compute D^η by restricting the calculation to the lowest-order

orthogonal polynomial, and by considering the high-temperature limit. We find

$$\eta_F = \begin{cases} \frac{5\sqrt{mT}}{32a^2\sqrt{\pi}}, & |a| \to 0, \\ \frac{15(mT)^{3/2}}{32\sqrt{\pi}}, & |a| \to \infty. \end{cases} \tag{41}$$

In the superfluid phase the shear viscosity is dominated by binary phonon scattering. The leading low-temperature behavior in the unitarity limit was calculated in [19]. Their result is

$$\eta_H = 5.06 \times 10^{-6} \xi^{7/2} \left(\frac{T_F}{T}\right)^5 \eta_0. \tag{42}$$

B. Prandtl number

The Prandtl number $\mathrm{Pr} = c_P \eta/(\rho\kappa)$ characterizes the relative importance of thermal and momentum diffusion. Here, ρ is the mass density of the fluid and c_P is the specific heat at constant pressure. In the high-temperature limit the specific heat can be calculated using the virial expansion, and at low temperature it can be computed using the effective phonon Lagrangian. The results are summarized in Appendix B. The leading term at high temperature is determined by the equation of state of an ideal gas of spin-up and -down atoms. In this limit we get $c_p = 5n/2$ and $\rho = mn$. The high-temperature limits of κ and η are given in Eq. (27) and Eq. (41). Putting these results together, we get

$$\mathrm{Pr} = 2/3, \quad T \gg T_F, \tag{43}$$

independent of the size of the scattering length. This result is remarkable because it implies that the Prandtl ratio agrees with the classical gas result even though the shear viscosity and thermal conductivity are not classical. This result can be traced to the fact that in the large-T limit the x and y integrals in Eqs. (24) and (39) factorize. The interaction depends only on y (related to the momentum transfer) and the leading y dependence of $\boldsymbol{B}_1 \cdot \boldsymbol{B}_1$ and $\hat{C}_0 \cdot \hat{C}_0$ is identical. This implies that both η and κ can be expressed in terms of the same transport cross section, and that there is no dependence on the scattering length in the Prandtl ratio. In Fig. 5 we plot the Prandtl number as a function of T/T_F for negative values of $k_F a$. As discussed in more detail in Appendix B, the virial expansion is smooth across the BCS-BEC transition, but our approximation for the bound state energy of the atom-atom dimer, $E_B = 1/(2ma^2)$, breaks down as we go too far toward the BEC side of the transition. For this reason we show the Prandtl number only for negative values of $k_F a$. We observe that the Prandtl number increases significantly as the temperature is lowered, and that it is only weakly dependent on $k_F a$.

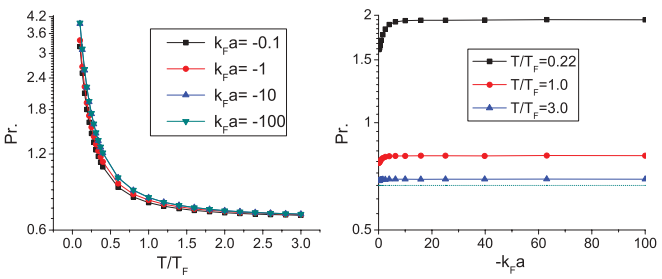

FIG. 5. (Color online) The left panel shows the Prandtl number as a function of T/T_F for different values of $k_F a$. The right panel shows the Prandtl number as a function of $k_F a$ for several values of T/T_F. The dashed line shows the high-temperature limit $\mathrm{Pr} = 2/3$.

V. SOUND ATTENUATION

Using the results for the shear viscosity and the thermal conductivity, we can also compute the sound attenuation coefficient. The intensity of a plane wave decreases as $e^{-2\gamma x}$, where $\gamma = \alpha\omega^2$ is the absorption coefficient and ω is the frequency of the wave. In the normal phase the parameter α is given by [35]

$$\alpha = \frac{\gamma}{\omega^2} = \frac{1}{2\rho c^3}\left[\frac{4}{3}\eta + \zeta + \rho\kappa\left(\frac{1}{c_V} - \frac{1}{c_P}\right)\right], \tag{44}$$

where ρ is the mass density of the fluid, c is the speed of sound, and ζ is the bulk viscosity. At unitarity $\zeta = 0$ and we can write

$$\alpha = \frac{2\eta}{3\rho c^3}\left(1 + \frac{3}{4}\frac{\Delta c_P}{\mathrm{Pr}}\right) \equiv \frac{\eta_0}{2\rho c^3}(\alpha_\eta^* + \alpha_\kappa^*), \tag{45}$$

where $\Delta c_P = (c_P - c_V)/c_V$ and $\eta_0 = (mT_F)^{3/2}$ as in Eq. (37). The quantities α_η^* and α_κ^* are plotted in Fig. 6.

In the high-temperature limit the Prandtl number is $\mathrm{Pr} \sim 2/3$ and $\Delta c_P \sim 2/3$. This implies that that the contribution to the sound attenuation coefficient due to thermal conductivity is 3/4 of the contribution due to shear viscosity. Also, both Pr and Δc_P are only weakly dependent on the scattering length; see Fig. 6. As the temperature is decreased the sound absorption coefficient is increasingly dominated by shear viscosity.

Below T_c there are two sound modes, ordinary (first) sound and second sound. The absorption coefficient for first sound is analogous to Eq. (44), except that the contribution from κ is absent. This implies that damping of first sound is entirely due to shear viscosity. The absorption coefficient of second sound is given by [36,37]

$$\alpha_2 = \frac{1}{2\rho c_2^3}\frac{\rho_s}{\rho_n}\left(\frac{4}{3}\eta + \zeta_2 - \rho(\zeta_1 + \zeta_4) + \rho^2\zeta_3 + \rho\frac{\rho_n}{\rho_s}\frac{\kappa}{c_P}\right), \tag{46}$$

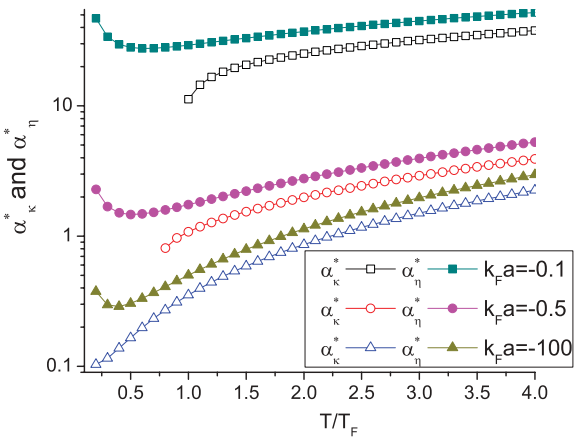

FIG. 6. (Color online) α_η^* and α_κ^* as functions of T/T_F. Note that the ratio of the two approaches a constant (3/4) as we go to larger values of T/T_F.

where $\rho_{n,s}$ are the normal and superfluid densities, c_2 is the speed of second sound, and ζ_i are the four different coefficients of bulk viscosity in the superfluid. Onsager's symmetry principle implies $\zeta_4 = \zeta_1$, and conformal symmetry requires that at unitarity $\zeta_1 = \zeta_2 = 0$. The remaining coefficient, ζ_3, vanishes as $\zeta_3 \sim T^3$ as the temperature goes to zero [21]. Using $\eta \sim 1/T^5$ and $\kappa \sim T^2$ we conclude that the damping of second sound is also dominated by shear viscosity.

We should note that at low temperature the phonon mean free path becomes very long, and the normal fluid ceases to behave hydrodynamically. A rough estimate of the relaxation times for shear viscosity and thermal conductivity is $\tau_\eta \simeq \eta/(nT)$ and $\tau_\kappa \simeq m\kappa/(c_P T)$. This implies that the relaxation time for shear viscosity grows very quickly, $\tau_\eta \sim 1/T^6$, whereas the relaxation time for thermal conductivity grows more slowly, $\tau_\kappa \sim 1/T^2$.

VI. CONCLUSIONS

In this work we studied the thermal conductivity of a dilute Fermi gas. Our main results are summarized in Fig. 4. We observe that the thermal conductivity scales as $\kappa \sim m^{1/2}T^{3/2}$ in the high-temperature limit and as $\kappa \sim m^{1/2}T_F^{3/2}(T/T_F)^2$ in the low-temperature limit. The Prandtl ratio equals 2/3 in the high-temperature limit, and increases as the temperature is lowered. This, together with the fact that $\Delta c_P = (c_P - c_V)/c_V$ decreases at low temperature, implies that the sound attenuation length in the strongly coupled normal fluid regime $T_c < T < T_F$ is dominated by shear viscosity. In order to assess the feasibility of measuring the sound attenuation length, we consider the ratio of wavelength λ to the attenuation length γ^{-1}. We find

$$\lambda\gamma = \frac{4\pi}{\sqrt{3\xi}}\left(\frac{k}{k_F}\right)\left(\frac{\eta}{n}\right)\left(1+\frac{3}{4}\frac{\Delta c_P}{\mathrm{Pr}}\right) \simeq 11.4\left(\frac{k}{k_F}\right)\left(\frac{\eta}{n}\right), \tag{47}$$

where we have used $\xi \simeq 0.44$ and $\Delta c_P/\mathrm{Pr} \simeq 0$. A rough estimate of the minimum value of η/n can be obtained by extrapolating the kinetic theory result down to $T = T_c$. We get

$$\left(\frac{\eta}{n}\right)_{\min} \simeq \frac{45\pi^{3/2}}{64\sqrt{2}}\left(\frac{T_c}{T_F}\right)^{3/2} \simeq 0.15. \tag{48}$$

Finally, we can express k/k_F in terms of the wavelength and the trap parameters. We obtain

$$\frac{k}{k_F} = \frac{R_z}{\lambda}\frac{\pi\beta^{2/3}}{(3N)^{1/3}}, \tag{49}$$

where R_z is the longitudinal cloud size, $\beta = R_\perp/R_z$ is the trap asymmetry, and N is the number of particles. For the experiment reported in [22] we get $k/k_F \simeq 0.046$ and $\lambda\gamma \simeq 0.08$. This implies that a measurement of the sound attenuation length is within reach. Higher sensitivity can be achieved by using more elongated traps or smaller wavelengths.

There are a variety of improvements that need to be made once experimental data become available. The most important is to replace the plane wave approximation that is the basis of Eq. (47) by a more detailed calculation of the wave profile in a given trap geometry. It will also be interesting to study attenuation of first and second sound in the superfluid phase.

ACKNOWLEDGMENTS

This work was supported in parts by the US Department of Energy Grant No. DE-FG02-03ER41260. We would like to thank C. Manuel, M. Mannarelli, and J. Thomas for useful discussions.

APPENDIX A: TRIAL FUNCTIONS

In this appendix we provide explicit expressions for some of the orthogonal polynomials and associated normalization constants. The orthogonality condition for the polynomials $B_s^{(F,H)}(x^2)$ is [see Eq. (21)]

$$A_s^{(F,H)}\delta_{st} = \int dx f_0(x)\,[1 \pm f_0(x)]x^4 B_s^{(F,H)}(x^2)B_t^{(F,H)}(x^2), \tag{A1}$$

where $B_0^{(F,H)}(x^2) = 1$ and

$$B_s^{(F,H)}(x^2) = x^{2s} + \sum_{i=0}^{s-1} a_{si}^{(F,H)}x^{2i} \tag{A2}$$

for $s \geqslant 1$. We will determine the coefficients $a_{si}^{(F,H)}$ iteratively. We define

$$c_n^{(F,H)} = \int dx f_0(x)\,[1 \pm f_0(x)]x^{4+n}, \tag{A3}$$

so that $A_0 = c_0$. We also find

$$\begin{aligned} a_{10} &= -c_2/c_0, \\ a_{20} &= \big(c_2c_6 - c_4^2\big)\big/\big(c_0c_4 - c_2^2\big), \\ a_{21} &= (c_0c_6 - c_2c_4)/\big(c_0c_4 - c_2^2\big), \\ &\vdots \end{aligned} \tag{A4}$$

and $A_1 = c_4 - c_2^2/c_0$. The integrals c_n depend on the quasiparticle dispersion relation. In the case of phonons with $E_p = vp$, we can evaluate A_1 to be

$$A_1^H = \frac{4\pi^4}{15}. \tag{A5}$$

In the case of the fermion with $E_p = p^2/2m$ and a chemical potential, we can only evaluate A_1 in the case of large temperature, which gives

$$A_1^F \simeq z\frac{15\sqrt{\pi}}{16}, \tag{A6}$$

where $z = e^{\mu/T}$ is the fugacity.

The orthogonal condition of the shear viscosity's trial function polynomials $\tilde{g}(x) = \sum c_s C_s(x^2)$ is different from that of thermal conductivity. Here, the polynomial is starting from the $s = 0$ term, since this set of polynomials satisfies the constraint of the momentum conservation law automatically (due to the tensor nature of the kernel for shear viscosity). The orthogonality condition is then

$$A_s^\eta\delta_{st} = \int dx f_0(x)\,[1 - f_0(x)]x^6 C_s(x^2)C_t(x^2), \tag{A7}$$

where the trial function $C_s(x^2) = x^{2s} + \sum_{i=0}^{s-1} a_{si}x^{2i}$. By the orthogonality condition Eq. (A7) and the same recursion

method that we used before, it is easy to get the coefficients a_{si} and also A_0^η, which is given by

$$A_0^\eta = \int dx f_0(x)\,[1 - f_0(x)]x^6 = z\int dx\; x^6 \frac{e^{x^2}}{\left(e^{x^2}+z\right)^2} \simeq z\frac{15\sqrt{\pi}}{16}, \tag{A8}$$

where the analytic result is valid in the high-temperature limit. Note that $A_1^F = A_0^\eta$ in the high-temperature limit; however, this is a mathematical coincidence coming from the similarity of the different integrals and the properties of the Γ function.

APPENDIX B: THERMODYNAMIC PROPERTIES

1. Virial expansion

In the high-temperature limit, $T \gg T_F$, the pressure can be expanded in powers of the fugacity $z = e^{\mu/T}$. This expansion is known as the virial expansion. We write

$$P(\mu,T) = \frac{\nu T}{\lambda^3}\sum_{l=1}^{\infty} b_l z^l, \tag{B1}$$

where $\lambda = \sqrt{2\pi/mT}$ is the thermal wavelength and ν is the spin degeneracy factor. The first virial coefficient is $b_1 \equiv 1$. The second virial coefficient was first calculated by Beth and Uhlenbeck [38]; see also [39,40]. Here we use these results in order to compute Δc_P. There are two contributions to b_2. The first is due to quantum statistics, which becomes important as $n\lambda^3 \sim 1$; the other is related to the atomic interaction. The correction due to quantum statistics is

$$b_l^0 = \begin{cases} l^{-5/2} & \text{(bosons)},\\ (-1)^{l+1} l^{-5/2} & \text{(fermions)}. \end{cases} \tag{B2}$$

The interacting contribution to the second virial coefficient is

$$b_2 - b_2^0 = \sqrt{2}\sum_n \left(e^{-\epsilon_n/T} - e^{-\epsilon_n^0/T}\right), \tag{B3}$$

where ϵ_n is the energy of the nth two-particle state in the center of mass frame and ϵ_n^0 is the corresponding noninteracting energy. In the universal regime these energies are determined by the scattering length only. We get [40]

$$b_2 - b_2^0 = \begin{cases} \frac{1}{\sqrt{2}}e^{x^2}[1 - \mathrm{erf}(|x|)], & x < 0,\\ \sqrt{2}e^{x^2} - \frac{1}{\sqrt{2}}e^{x^2}[1 - \mathrm{erf}(x)], & x > 0, \end{cases}$$

where $\mathrm{erf}(x)$ is the error function, $x = \lambda/(a\sqrt{2\pi})$, and the bound state energy in the $x > 0$ case was assumed to be $E_B = 1/(ma^2)$. We can write down the asymptotic forms in the limits of zero and infinite scattering lengths as

$$b_2 - b_2^0 = \begin{cases} -\frac{a}{\lambda}, & a \to 0^-,\\ \sqrt{2}e^{1/(mTa^2)}, & a \to 0^+,\\ \frac{1}{\sqrt{2}}\left(1 + \frac{\sqrt{2}}{\pi}\frac{\lambda}{|a|}\right), & a \to \pm\infty. \end{cases} \tag{B4}$$

The interaction part of b_2 approaches a finite value as $a \to \infty$, and is of the same order as the effects of quantum statistics. One can also see that the total b_2 will start off negative for small and negative scattering length, but eventually becomes positive as $a \to -\infty$. This implies that there is a value of the scattering length for which the effects of the interaction and of quantum statistics cancel. For positive scattering lengths, the contribution of the interaction is positive and always larger than the quantum correction, so that $b_2 > 0$ for all $a > 0$. In the BEC limit ($a \to 0^+$) the binding energy of the bound state is large and b_2 becomes large also. In this limit, however, universality breaks down and the binding energy cannot be expressed in terms of the scattering length only.

2. Specific heat

The specific heat can be expressed in terms of partial derivatives of the pressure. The independent thermodynamic variables are (μ,T). The first derivatives with respect to these variables determine the entropy density and pressure:

$$s = \left.\frac{\partial P}{\partial T}\right|_\mu, \quad n = \left.\frac{\partial P}{\partial \mu}\right|_T. \tag{B5}$$

In order to compute the specific heat at constant volume, we use $V = N/n$ and write

$$c_V = T\left.\frac{\partial s}{\partial T}\right|_V = \frac{\partial(s,V)}{\partial(T,V)} = \frac{\partial(s,V)/\partial(T,\mu)}{\partial(T,V)/\partial(T,\mu)} = T\left(\left.\frac{\partial s}{\partial T}\right|_\mu - \frac{[(\partial n/\partial T)|_\mu]^2}{(\partial n/\partial\mu)|_T}\right), \tag{B6}$$

where the Jacobian is defined as

$$\frac{\partial(a,b)}{\partial(c,d)} = \mathrm{Det}\begin{pmatrix} \partial a/\partial c|_d & \partial a/\partial d|_c \\ \partial b/\partial c|_d & \partial b/\partial d|_c \end{pmatrix}.$$

In order to compute c_P we make use of the relation between $c_P - c_V$ and the thermal expansion coefficient $(1/V)(\partial V/\partial T)|_P$. This relation is given by

$$c_P - c_V = -T\frac{[(\partial V/\partial T)|_P]^2}{(\partial V/\partial P)|_T}. \tag{B7}$$

The partial derivatives are

$$\left.\frac{\partial V}{\partial T}\right|_P = \frac{s}{n}\left.\frac{\partial n}{\partial \mu}\right|_T - \left.\frac{\partial n}{\partial T}\right|_\mu, \quad \left.\frac{\partial V}{\partial P}\right|_T = \left.\frac{\partial n}{\partial \mu}\right|_T, \tag{B8}$$

which gives

$$c_P = c_V + T\frac{\left[\frac{s}{n}(\partial n/\partial\mu)|_T - (\partial n/\partial T)|_\mu\right]^2}{(\partial n/\partial\mu)|_T}. \tag{B9}$$

a. High-temperature phase

In the high-temperature phase we use the virial expansion of the pressure including terms up to second order, $P = \frac{\nu T}{\lambda^3}(z + b_2 z^2)$. Using the results of the previous section, we find

$$c_V = \frac{\nu z}{\lambda^3}\left(\frac{3}{2} + \frac{15}{4}zb_2 - zT\frac{\partial b_2}{\partial T} + zT^2\frac{\partial^2 b_2}{\partial^2 T}\right), \qquad c_P = c_V + \frac{\nu z}{\lambda^3}\left(1 + 5zb_2 - 2zT\frac{\partial b_2}{\partial T}\right). \tag{B10}$$

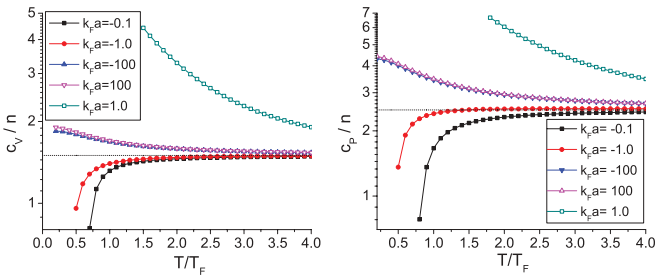

FIG. 7. (Color online) The left panel shows c_V in units of n_0 as a function of T/T_F n_0. Here, $n_0 = \nu z/\lambda^3$ is the density of the free gas. The right panel shows the temperature dependence of c_P.

We recover the result for a classical noninteracting gas by setting $b_2 = 0$ and $n = \frac{\nu z}{\lambda^3}$. We show the result for an interacting gas in Fig. 7. We observe that the results are smooth across the BCS-BEC transition. We note, however, that on the BEC side the virial expansion breaks down at temperatures larger than the Fermi temperature. This is related to the presence of a deeply bound state.

b. Superfluid phase

At zero temperature the pressure is given by

$$P = \frac{4\sqrt{2}}{15\pi^2\xi^{3/2}} m^{3/2}\mu^{5/2}, \tag{B11}$$

and the density is

$$n = \left.\frac{\partial P}{\partial \mu}\right|_T = \frac{2\sqrt{2}m^{3/2}}{3\pi^2\xi^{3/2}}\mu^{3/2}. \tag{B12}$$

The leading low-temperature correction arises from phonons. The phonon contribution to the pressure is

$$P_H = \frac{\pi^2 T^4}{90}\left(\frac{3m}{2\mu}\right)^{3/2}. \tag{B13}$$

Using these results, we find

$$\begin{aligned} c_V &= \frac{2\pi^2 T^3}{15}\left(\frac{3m}{2\mu}\right)^{3/2} + O(T^7), \\ c_P &= c_V + O(T^7). \end{aligned} \tag{B14}$$

These results imply that Δc_p vanishes at low temperature much faster than c_P and c_V.

[1] I. Bloch, J. Dalibard, and W. Zwerger, Rev. Mod. Phys. **80**, 885 (2008).
[2] S. Giorgini, L. P. Pitaevskii, and S. Stringari, Rev. Mod. Phys. **80**, 1215 (2008).
[3] T. Schäfer and D. Teaney, Rep. Prog. Phys. **72**, 126001 (2009).
[4] K. M. O'Hara, S. L. Hemmer, M. E. Gehm, S. R. Granade, and J. E. Thomas, Science **298**, 2179 (2002).
[5] S. S. Adler *et al.* (PHENIX Collaboration), Phys. Rev. Lett. **91**, 182301 (2003).
[6] B. B. Back *et al.* (PHOBOS Collaboration), Phys. Rev. C **72**, 051901 (2005).
[7] J. Adams *et al.* (STAR Collaboration), Phys. Rev. C **72**, 014904 (2005).
[8] T. Schäfer, Phys. Rev. A **76**, 063618 (2007).
[9] A. Turlapov, J. Kinast, B. Clancy, L. Luo, J. Joseph, and J. E. Thomas, J. Low Temp. Phys. **150**, 567 (2008).
[10] T. Schäfer and C. Chafin, e-print arXiv:0912.4236 [cond-mat. quant-gas].
[11] K. Dusling and D. Teaney, Phys. Rev. C **77**, 034905 (2008).
[12] P. Romatschke and U. Romatschke, Phys. Rev. Lett. **99**, 172301 (2007).
[13] G. Policastro, D. T. Son, and A. O. Starinets, Phys. Rev. Lett. **87**, 081601 (2001).
[14] D. T. Son and A. O. Starinets, Annu. Rev. Nucl. Part. Sci. **57**, 95 (2007).
[15] J. M. Maldacena, Adv. Theor. Math. Phys. **2**, 231 (1998); Int. J. Theor. Phys. **38**, 1113 (1999).
[16] D. T. Son, Phys. Rev. D **78**, 046003 (2008).
[17] K. Balasubramanian and J. McGreevy, Phys. Rev. Lett. **101**, 061601 (2008).
[18] G. M. Bruun and H. Smith, Phys. Rev. A **72**, 043605 (2005).
[19] G. Rupak and T. Schäfer, Phys. Rev. A **76**, 053607 (2007).
[20] D. T. Son, Phys. Rev. Lett. **98**, 020604 (2007).
[21] M. A. Escobedo, M. Mannarelli, and C. Manuel, Phys. Rev. A **79**, 063623 (2009).
[22] J. Joseph, B. Clancy, L. Luo, J. Kinast, A. Turlapov, and J. E. Thomas, Phys. Rev. Lett. **98**, 170401 (2007).
[23] E. Taylor, H. Hu, X.-J. Liu, L. P. Pitaevskii, A. Griffin, and S. Stringari, Phys. Rev. A **80**, 053601 (2009).
[24] E. Burovski, N. Prokof'ev, B. Svistunov, and M. Troyer, Phys. Rev. Lett. **96**, 160402 (2006).
[25] D. T. Son and M. Wingate, Ann. Phys. **321**, 197 (2006).
[26] J. Carlson, S.-Y. Chang, V. R. Pandharipande, and K. E. Schmidt, Phys. Rev. Lett. **91**, 050401 (2003).
[27] G. Rupak and T. Schäfer, Nucl. Phys. A **816**, 52 (2009).
[28] A. M. J. Schakel, e-print arXiv:0912.1955v1 [cond-mat.quant-gas].
[29] R. Haussmann, M. Punk, and W. Zwerger, Phys. Rev. A **80**, 063612 (2009).
[30] L. Salasnich and F. Toigo, Phys. Rev. A **78**, 053626 (2008).
[31] M. Braby, J. Chao, and T. Schäfer, Phys. Rev. C **81**, 045205 (2010).
[32] G. M. Bruun and H. Smith, Phys. Rev. A **75**, 043612 (2007).
[33] T. R. Kirkpatrick and J. R. Dorfman, J. Low Temp. Phys. **58**, 301 (1985).
[34] P. C. Hohenberg and B. I. Halperin, Rev. Mod. Phys. **49**, 435 (1977).
[35] L. D. Landau and E. M. Lifshitz, *Fluid Dynamics*, Course of Theoretical Physics Vol. VI (Pergamon Press, Oxford, 1959).
[36] J. Wilks, *The Properties of Liquid and Solid Helium* (Clarendon, Oxford, 1966).
[37] S. J. Putterman, *Superfluid Hydrodynamics* (North-Holland, Amsterdam, 1974).
[38] G. E. Uhlenbeck and E. Beth, Physica **3**, 729 (1936).
[39] T.-L. Ho and E. J. Mueller, Phys. Rev. Lett. **92**, 160404 (2004).
[40] D. Lee and T. Schäfer, Phys. Rev. C **73**, 015201 (2006).